2958–2968 *Nucleic Acids Research, 2008, Vol. 36, No. 9* *Published online 3 April 2008*
doi:10.1093/nar/gkn045

A shared RNA-binding site in the Pet54 protein is required for translational activation and group I intron splicing in yeast mitochondria

Benjamin J. Kaspar, Abby L. Bifano and Mark G. Caprara*

Center for RNA Molecular Biology, Case Western Reserve University, School of Medicine, Cleveland, OH 44106-4960, USA

Received November 30, 2007; Revised January 23, 2008; Accepted January 24, 2008

ABSTRACT

The Pet54p protein is an archetypical example of a dual functioning ('moonlighting') protein: it is required for translational activation of the COX3 mRNA and splicing of the aI5β group I intron in the COX1 pre-mRNA in *Saccharomyces cerevisiae* mitochondria (mt). Genetic and biochemical analyses in yeast are consistent with Pet54p forming a complex with other translational activators that, in an unknown way, associates with the 5′ untranslated leader (UTL) of COX3 mRNA. Likewise, genetic analysis suggests that Pet54p along with another distinct set of proteins facilitate splicing of the aI5β intron, but the function of Pet54 is, also, obscure. In particular, it remains unknown whether Pet54p is a primary RNA-binding protein that specifically recognizes the 5′ UTL and intron RNAs or whether its functional specificity is governed in other ways. Using recombinant protein, we show that Pet54p binds with high specificity and affinity to the aI5β intron and facilitates exon ligation *in vitro*. In addition, Pet54p binds with similar affinity to the COX3 5′ UTL RNA. Competition experiments show that the COX3 5′UTL and aI5β intron RNAs bind to the same or overlapping surface on Pet54p. Delineation of the Pet54p-binding sites by RNA deletions and RNase footprinting show that Pet54p binds across a similar length sequence in both RNAs. Alignment of the sequences shows significant (56%) similarity and overlap between the binding sites. Given that its role in splicing is likely an acquired function, these data support a model in which Pet54p's splicing function may have resulted from a fortuitous association with the aI5β intron. This association may have lead to the selection of Pet54p variants that increased the efficiency of aI5β splicing and provided a possible means to coregulate COX1 and COX3 expression.

INTRODUCTION

Group I introns are mobile genetic elements that have colonized diverse sets of organisms including bacteria, bacteriophage and unicellular eukaryotes (1). As one example, the mitochondria (mt) of *Saccharomyces cerevisiae* contain up to nine group I introns that are found within the cytochrome oxidase (COX) 1, apocytochrome b (COB) and large ribosomal RNA genes (2). While some group I introns can self-splice *in vitro*, most are believed to require proteins for splicing *in vivo*. In fact, genetic analysis in fungi has shown that a number of nuclear encoded mt proteins are required for group I intron splicing. In most cases, individual proteins show high substrate specificity and facilitate splicing of only one intron. Interestingly, in a few specific cases, these proteins have additional mt functions, such as aminoacylation or translational activation, and splicing function likely reflects the secondary adaptation of each protein (3). Thus, investigations of such group I intron cofactors provides a rich opportunity to understand details of molecular evolution that may be pertinent in the selection of other multifunctional ('moonlighting') proteins in more complex organisms, such as pre-mRNA splicing cofactors which are secondarily involved in mRNA export and translational regulation (4,5).

The Pet54p protein is an intriguing example of a nuclear encoded moonlighting protein in yeast mt. Disruption of the *PET54* gene affects both the processing of the aI5β group I intron in the COX1 pre-mRNA and the translation of the COX3 mRNA (6,7). Despite extensive investigations, the mechanisms of Pet54p function in these two unrelated processes remains elusive.

*To whom correspondence should be addressed. Tel: +216 368 4757; Fax: +216 368 2010; Email: mgc3@po.cwru.edu

In particular, it is unknown whether Pet54p is a primary RNA-binding protein that specifically recognizes both RNAs or whether its functional specificity is governed in other ways.

Pet54p is a small, ~35-kDa protein that contains an RNA recognition motif (RRM) near its C-terminus. Genetic and biochemical analyses have established that Pet54p interacts with two other factors, Pet122 and Pet494, and this complex functionally interacts with the 5′ untranslated leader (UTL) of COX3 mRNA. The multipart complex is essential for COX3 translation, since disruption of any component severely reduces COX3 protein production (8,9). How the complex assembles on the 5′ UTL and promotes translation is not known, but, once bound, it may serve to facilitate ribosome recognition of the AUG start codon (9–11). The presence of an RRM in Pet54p is suggestive that the protein binds to the 5′ UTL of COX3, but no direct evidence exists to show this is the case. However, deletions within the COX3 5′ UTL exacerbate the respiratory-deficient (mt-impaired) phenotype of a mis-sense mutation just downstream of the RRM motif in Pet54p. These observations are thought to reflect a functional interaction between Pet54p and RNA (8).

The role of Pet54p in promoting aI5β splicing is even less clear. Like all group I introns, the aI5β intron must fold into an active conformation to catalyze the self-splicing reaction (12,13). Genetic analyses have shown that aI5β splicing efficiency is reduced when one of five mt targeted nuclear genes, including PET54, is disrupted (3,6). An attractive hypothesis is that Pet54p along with the other proteins function to facilitate folding of the intron. Protein involvement in group I intron folding has been demonstrated *in vitro* for the *Neurospora crassa* mt tyrosyl tRNA synthetase, *S. cerevisiae* mt CBP2 and *Aspergillus nidulans* I-AniI proteins (14–17). The disruption of the PET54 gene does not appear to affect the splicing of any other yeast mt group I intron suggesting that the protein may interact directly with the aI5β intron or one of its other cofactors (6).

As a starting point to understand how Pet54p functions as both an activator of COX3 translation and as an essential cofactor in the splicing of aI5β intron, we have analyzed its interaction with both RNA ligands using recombinant Pet54p purified from bacteria. UV cross-linking experiments provide evidence that Pet54p specifically recognizes both the COX3 5′ UTL and the COX1 pre-mRNA containing the aI5β intron. *In vitro* experiments are consistent with Pet54p facilitating the exon ligation step of aI5β splicing. Competition experiments show that both COX3 5′ UTL and aI5β containing pre-RNA bind to the same or overlapping sites in Pet54p. RNA mapping and mutational experiments demonstrate that Pet54p binds to regions in each RNA that share sequence similarity. Collectively, these observations are consistent with Pet54p using analogous interactions to bind both RNAs and support a model in which a fortuitous association with the aI5β intron provided the opportunity by which Pet54p adapted to function in splicing.

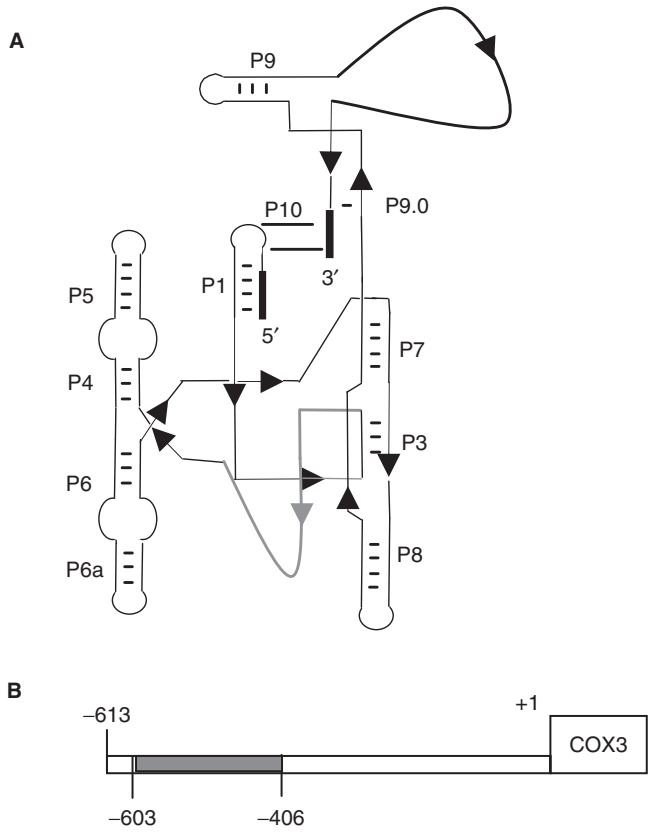

Figure 1. Schematic of Pet54p RNA ligands. (**A**) Secondary structure model of COX1 aI5β intron RNA. The noncanonical sequence inserted ('insertion sequence') between P3 and P4 is shaded in gray. (**B**) Schematic of the COX3 5′ UTL. Gray shading represents a region of the UTL that was previously deleted resulting in loss of translational activation (23; see text). Note that the 5′ UTL is numbered relative to the start of the coding region (+1).

MATERIALS AND METHODS

Molecular cloning and mutagenesis

The aI5β intron containing *COX1* gene was amplified from mt genomic DNA isolated from the BY4741 yeast strain using the primers AI5Top (5′-GCGGAATTCTAA TACGACTCACTATAGGGATCCACGATATTAATT TAATAAGTGTCG TGC) and AI5Bot (5′-GGAAGCT TCACCACGTAGTAAGTCATAAAAAAAAAAG) to make paI5FL. The downstream truncated aI5β intron construct (paI5Prox) was made using AI5Top primer and the AI5 Prox (5′-GGAAGCTTCAACTTTATTATTAGT TAATTA), which hybridized just downstream of the catalytic core of aI5β (see Figure 1). The COX3 5′ UTL was also amplified from mt genomic DNA using the primers T7COX3UTL (5′- GCGGAATTCGCAGTA ATACGACTCACTATAGGGTTCGAACCCTATATT TACTAAA) and COX3UTLBOT (5′-GGAAGCTTCTT GATGTCTACTTCTTTCTAAATGTGTCAT) to make pCOX3UTL. Each PCR product contained a T7 RNA polymerase promoter for *in vitro* transcription. The PCR products were cloned in pGFP UV vector (Clontech, Mountain View, CA., USA). The aI5β and UTL constructs were sequenced completely.

PCR templates were used to generate transcripts containing RNA subdomains. For aI5β, the P1 + INS template was amplified from paI5Prox using AI5Top and Delta P4-5Bot (5′-GGAAGCTTATAATTATAAGAG TTTCCCCGTTTA), while the P3-3E template was amplified from a version of paI5FL deleted for the large insertion sequence downstream of P1 using Delta P1Top (5′-GCGGAATTCTAATACGACTCACTATAGGGTG TCGTGCTTAAAATTCACTA) and AI5 Prox. For COX3UTL, the COX3UPST template was amplified from pCOX3UTL using primers T7COX3UTL and 8A1(5′-CTCTTTCGACCGGATTATTTATTC), while the COX3DNST template was amplified from pCOX3UTL using primers 8A2 (5′-GGTAATACGACT CACTATAGGGAGAGAATAAATAATCCGGTCGA AAGAG) and COX3UTLBOT.

The *PET54* gene was amplified from genomic DNA using the primers PET54Top (5′-CCGGATCCGATG AAGGCTTCTAGTAAAGCTATTA) and PET54Bot (5′-GGAAGCTTTTCACTAAGATGTTCAATTAATA). The PCR product was cloned into the pet28b vector (EMD Biosciences, Inc., San Diego, CA, USA) downstream of a His6 tag that was used for protein purification. The Pet54p expression clone was sequenced completely.

Protein expression and purification

Initial experiments showed that recombinant Pet54p was largely insoluble when expressed in *E. coli* and so protein purification was performed under denaturing conditions. Recombinant Pet54p was expressed and purified essentially as described previously for the I-AniI protein (19) with the following exceptions. The lysis, wash and elution buffers contained 6 M guanidine-HCl. The eluted protein was renatured by dialysis against a series of buffers containing decreasing concentrations of guanidine-HCl. The final dialysis was against 20 mM Tris–HCl, pH 7.9, 500(or 100) mM NaCl and 50% glycerol. The protein was stored at −20°C. Protein concentration was determined by absorption at 279 nm in 6 M guanidine-HCl, 20 mM Na-phosphate buffer, pH 6.5 using the calculated extinction coefficient of 43 320 $M^{-1}cm^{-1}$. A small contaminating peptide (~7 kDa) was present in each preparation and the A_{279} value was corrected for its presence prior to calculating the Pet54p concentration.

For filter binding and RNA footprinting experiments, Pet54p lacking the first 20 amino acids (Pet54Δ20p) of its N-terminus was used. This truncation results in more soluble protein allowing for purification under native conditions. Both Pet54Δ20p and recombinant Mrs1p were purified as described previously for the I-AniI protein with the exception that Pet54Δ20p was expressed at 16°C for 20 h (18).

RNA transcription and purification

All plasmids were digested with HindIII. Transcription reactions were in 50 or 100 µl of reaction medium containing 2–5 µg of plasmid DNA, 5 U/µl phage T7 RNA polymerase, 25 mM NaCl, 8 mM $MgCl_2$, 40 mM Tris–HCl, pH 8.0, 2 mM spermidine, 10 mM dithiothreitol (DTT), 0.5–1 mM NTPs and 1 U/µl RNase OUT (Promega, Madison, WI, USA) for 60–120 min at 37°C. ^{32}P-labeled transcripts used in cross-linking experiments were synthesized by adding 1 µCi/µl [α-^{32}P]UTP (3000 Ci/mmol; ICN Biomedicals, Irvine, CA, USA) to a transcription mix containing 0.5 mM 4-thioUTP (Ambion, Austin, TX, USA), 0.5 mM UTP, 1 mM of each remaining NTP. High specific-activity transcripts used in filter-binding experiments were synthesized by adding 4 µCi/µl [α-^{32}P]UTP (3000 Ci/mmol; ICN Biomedicals) to a transcription mix containing 0.04 mM UTP, 0.4 mM of each remaining NTP.

To generate end-labeled adenosine- or cytosine-phosphorothioate containing RNAs, the transcription mix included 1 mM guanosine, 0.025 mM ATPαS or 0.063 mM CTPαS (Glenn Research, Sterling, VA, USA) along with the remaining nucleotide triphosphates. For all synthesis reactions, after transcription, the DNA template was digested with DNase I (0.5 U/µl; FPLC-purified; Pharmacia Biotech Inc., Piscataway, NJ, USA) for 20 min at 37°C. Transcripts were extracted with phenol-chloroform-isoamyl alcohol (phenol-CIA; 25:24:1 v/v/v), centrifuged through a Sephadex G-50 (Sigma Chemical Co., St Louis, MO, USA) spun column. Unsubstituted transcripts were prepared similarly but without phosphorothioate triphosphates.

Transcripts were 5′ end-labeled as described (17). The end-labeled and high specific-activity transcripts were further purified by denaturing gel electrophoresis. For all experiments, prior to use, RNA was heated to 90°C in H_2O for 20 s and placed on ice.

UV cross-linking

For the cross-linking experiments, internally ^{32}P-labeled 4-thiouridine containing transcript (20 nM) was incubated in the absence or presence of Pet54p (~250 nM) in 50 mM Tris–HCl, pH 7.5, 100 mM NaCl and 7 mM $MgCl_2$ (TNM buffer) for 10 min. For competition experiments, unlabeled competitor RNAs were included at a final concentrations of 50 to 750 nM (see Figures 2 and 3 legends). The reaction mixture was then placed in a 96-well plate on ice and irradiated at 312 nm in a UV Stratalinker 1800 (Stratagene, La Jolla, CA, USA) for 20 min. A ribonuclease cocktail of RNaseA and T1 was added (Worthington Biochemical Corp., Lakewood, NJ, USA) and the RNA was digested for 60 min at 42°C. The products were separated on a 10% SDS–PAGE gel. The dried gels were visualized with a phosphorimager (Amersham Biosciences, Piscataway, NJ, USA) or exposure to X-ray film. All experiments were repeated with identical results.

RNA splicing assays

5′-^{32}P-end-labeled aI5β pre-RNA was incubated in TMN buffer supplemented with 2 mM spermidine, 10 mM DTT, 0.7 U/µl of RNase OUT, 1 mM GTP and 0.7 µg/µl tRNA for 5 min at 37°C. Pet54p (final concentration, ~250 nM) and/or Mrs1p (final concentration 1 µM) were added to initiate the splicing reaction. Aliquots were removed at increasing times and the reaction quenched with 1 µl of 0.5 M EDTA (pH 8.0) and extraction with phenol-CIA.

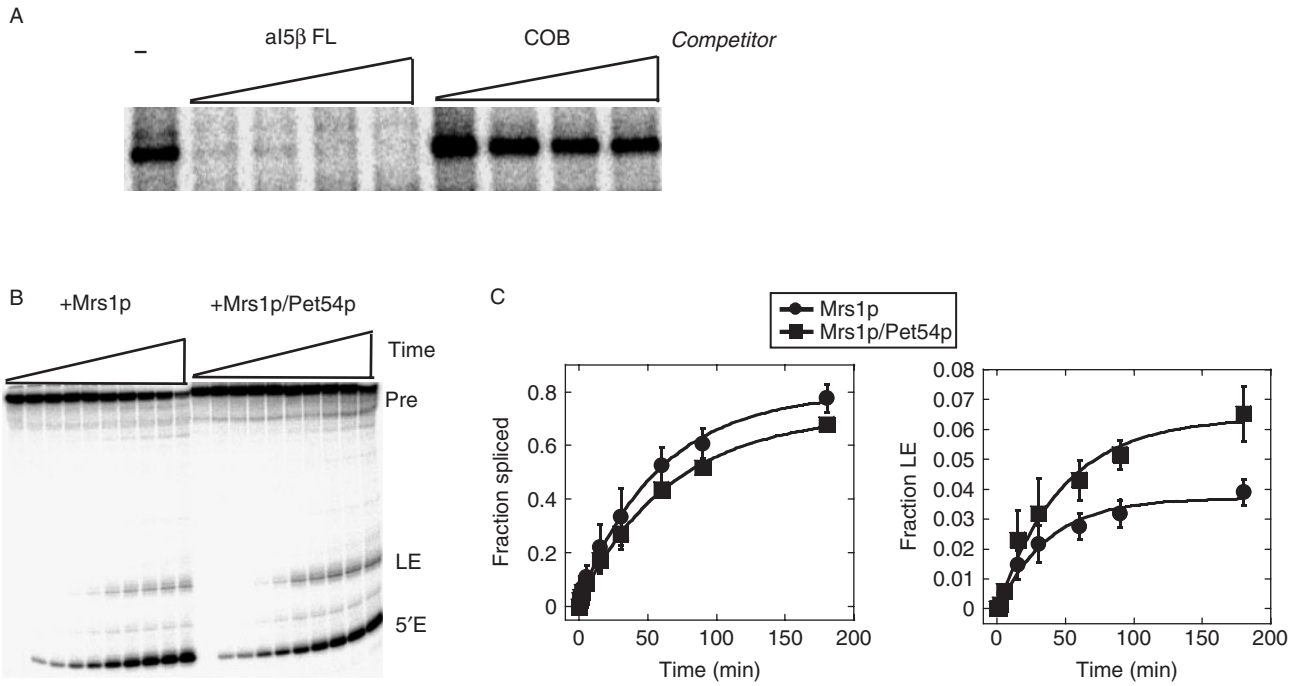

Figure 2. Pet54p binds directly to the aI5β pre-RNA and facilitates exon ligation. (**A**) UV cross-linking. Internally ^{32}P-radiolabeled 4-thiouridine containing aI5β pre-RNA (20 nM) was incubated with Pet54p in the presence of increasing concentrations (50–750 nM) competitor RNA. After irradiation at 312 nm, the RNA was digested with ribonucleases and the reactions electrophoresed through an SDS–PAGE gel. Radiolabeling of Pet54p indicates a cross-link with the RNA. aI5β FL, full-length aI5β pre-RNA; COB, *A. nidulans* mt COB group I intron pre-RNA (**B**) Time course of Pet54p facilitated exon ligation. 5′-^{32}P-labeled aI5β pre-RNA was incubated with 1 μM Mrs1p with or without 250 nM Pet54p. (**C**) Plots of the total fraction RNA spliced and fraction of ligated exon (LE) produced. The data are averages from two independent experiments and the error bars represent standard deviations. The data were fit to the first-order equation: Fraction RNA species = A $(1 - e^{-kt})$ where A is the amplitude of RNA processed and k represents the pseudo-first-order rate constant, k_{obs}. A third experiment with a different preparation of RNA also yielded a1.5-fold increase in exon ligation. Titration experiments confirmed that the concentration of Pet54p was saturating for these experiments (see also Figure 4).

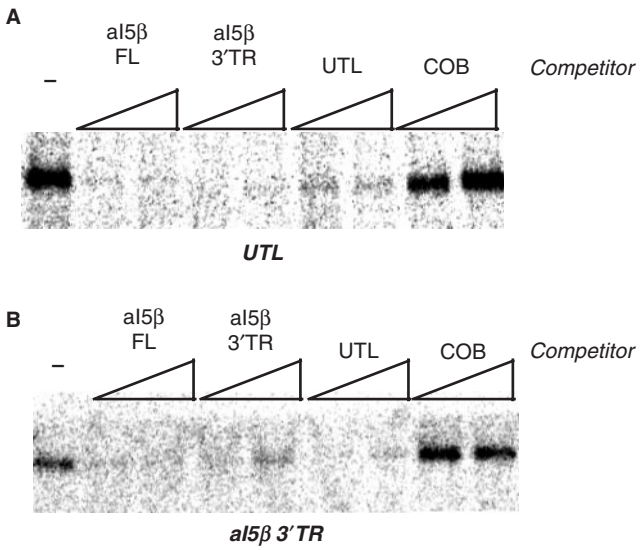

Figure 3. Specific binding of Pet54p to the COX3 5′ UTL and aI5β pre-RNA. Internally ^{32}P-radiolabeled 4-thiouridine containing 5′ UTL (**A**) or aI5β pre-RNA (**B**) was incubated with Pet54p in the absence or presence of increasing amounts of unlabeled competitor RNAs (250 and 500 nM). aI5β FL, full-length aI5β pre-RNA; aI5β 3′ TR, aI5β pre-RNA truncated after the P9.1 structure (see Figure 1); UTL, COX3 5′ UTL; COB, *A. nidulans* mt COB group I intron pre-RNA.

The reaction products were separated in a denaturing 10% polyacrylamide/7 M urea/5% glycerol gel and the dried gels were visualized with a phosphorimager. Titration experiments confirmed that the concentrations of Mrs1p and Pet54p were saturating for these experiments.

Delineation of Pet54p-binding sites

For boundary experiments, 5′- ^{32}P-labeled phosphorothioate substituted RNA was cleaved with iodine (80 nM final concentration) for 10 min at 42°C. Iodine was removed by ethanol precipitation and the RNA resuspended in water. For T1 digestion, nonsubstituted 5′- ^{32}P-labeled RNA was cleaved with T1 (5 U; Ambion) for 10 min at 50°C, extracted with phenol-CIA, ethanol precipitation and the RNA resuspended in water. Pet54p (~250 nM) and RNA (10 nM) were incubated in TNM buffer at 37°C for 5 min and then filtered through a nitrocellulose filter that was subsequently washed with 3 ml of TNM buffer. Pet54p-bound RNA was recovered by extraction of the filter with phenol-CIA and ethanol precipitation. The products were separated in a denaturing 6% polyacrylamide/7 M urea gel and the dried gels were visualized with a phosphorimager. The experiments were repeated with identical results.

RNA binding

For K_d measurements, ~2 pM ^{32}P-labeled RNA was incubated with 0 to 500 nM Pet54p in 50 µl TMN buffer containing 0.25 µg/µl heparin and 0.1 µg/µl bovine serum albumin at 37°C. The complexes were filtered after 30 min through nitrocellulose (BA85; Schleicher and Schuell, Keene, NH, USA), washed with 3 ml of buffer, dried and counted using a Beckman-Coulter LS6500 scintillation counter (Beckman-Coulter Inc., Fullerton, CA, USA). The data were fit to the following equation: Fraction RNA bound = $A \times E/(E + K_d^{app})$ where A is the total amplitude bound and E is the concentration of Pet54p and K_d^{app} is the apparent equilibrium binding constant. Each titration was repeated two to four times and errors are expressed as standard deviations.

RNA footprinting

5′end-labeled transcripts (~3 nM) were incubated in the absence or presence of Pet54p (1.25 or 2.5 µM) in TNM buffer plus 10 ng/µl *E. coli* tRNA at 37°C for 10 min. Aliquots (15 µl) were treated with either buffer, RNase 1 (2.1 U, Ambion) or RNase V1 (0.012 U, Ambion) for 20 s and the reactions stopped by addition of 2 µl of aurin tricarboxylic acid, 1 µl of 0.5 M EDTA and extraction with phenol-CIA. The products were separated in a series of denaturing 6% polyacrylamide/7 M urea gel and the dried gels were visualized and quantified with a phosphorimager. The bands were identified based on comigration with RNase T1 and random hydrolysis markers. Because single nucleotide resolution is more difficult with fragments larger than 150 nt, the assignment of the ends of larger fragments may be 2 or 3 nt displaced. The data were analyzed by subtracting background (based on mock-treated control samples) and band intensities were normalized for each lane with respect to the precursor RNA to account for any loading differences in each lane. Residues were scored protected by Pet54p if the band intensity was <50% of those in the absence of protein (17).

RESULTS

Cloning PET54, the 5′ UTL of COX3 and aI5β containing pre-RNA into expression vectors

The *PET54* gene was amplified by PCR from yeast genomic DNA and cloned into a bacterial expression vector. The construct contained a short His6-tag fused to the N-terminus of Pet54 that was used to purify the protein using affinity chromatography (see Materials and Methods section). The 613-nt 5′ UTL of COX3 along with the upstream tRNA^{val} gene and the aI5β intron with flanking exon sequences were amplified by PCR and cloned into a vector downstream of a T7 RNA polymerase promoter for use in generating RNAs via *in vitro* transcription (see Materials and Methods section). The COX3 5′ UTL is numbered relative to the first base (+1) of the mRNA coding region: 5′ end of the leader is designated −613 and the last base is −1 (7). The 1604-nt aI5β pre-RNA includes a 12-nt 5′ exon, the catalytic core, an open reading frame encoding a degenerate homing endonuclease and the 3′ splice site (SS) followed by an 18-nt 3′ exon (Figure 1). Notably, the aI5β intron contains a noncanonical 162-nt AU-rich insertion sequence that interrupts the normally 3-nt J3/4 sequence between the 5′ strands of P3 and P4 (Figure 1). To facilitate *in vitro* transcription yield, we also created a shorter RNA that contained the 5′ exon and catalytic core followed by a short sequence extension (aI5β 3′TR pre-RNA). Equilibrium binding experiments demonstrated that Pet54p has the same affinity for the truncated and full-length aI5β pre-RNAs (data not shown), and we used this RNA for some of the experiments described below.

Pet54p specifically associates with aI5β RNA and facilitates the exon ligation step of splicing *in vitro*

To test if recombinant Pet54p was capable of binding the aI5β pre-RNA in the absence of other splicing cofactors, we performed UV cross-linking experiments. Internally labeled, 4-thiouridine containing RNAs were incubated with Pet54p, exposed to UV light, the RNA degraded by RNases and the products separated by SDS–PAGE. As shown in Figure 2A, Pet54p was cross-linked with the aI5β pre-RNA in this assay. Control experiments showed that the crosslink was dependent on 4-thiouridine substitution and UV irradiation (data not shown). Some group I intron cofactors recognize conserved structural features in group I introns and thus binds to multiple introns indiscriminately (3). To test the specificity of the Pet54p interaction, unlabeled group I intron competitor RNAs were included in the cross-linking reactions. Figure 2A shows that inclusion of full-length aI5β pre-RNA significantly decreased cross-linking efficiency. In contrast, the presence of the mt COB group I intron RNA from *A. nidulans* did not decrease cross-linking efficiency. Like the aI5β intron, the COB intron transcript is AU rich (65%) and folding studies suggest that almost all of the conserved secondary structure elements are formed in this intron (17). These data suggest that cross-linking is reporting a specific interaction between Pet54p and the aI5β pre-RNA and, furthermore, Pet54p does not recognize conserved secondary structural features in group I introns.

We have recently developed an *in vitro* splicing assay with the aI5β intron and the Mrs1p protein (A.L. Bifano and M.G. Caprara, in preparation). The aI5β intron does not self-splice *in vitro* under near physiological concentrations of divalent cations (7 mM Mg^{2+}). However, binding of recombinant Mrs1p protein efficiently facilitated the first step of aI5β splicing *in vitro* (A.L. Bifano and M.G. Caprara, in preparation; Figure 2B). A plot of the fraction of pre-RNA spliced versus time showed that the first step occurred with a rate of 0.02(±0.005) min^{-1}. However, the fraction of RNA that underwent the second step was only 0.04 (±0.009) after 3 h and may reflect that the 3′SS was not properly positioned in the aI5β catalytic core or the intron did not undergo the appropriate conformational changes required for the exon ligation [e.g. (19,20)]. Addition of Pet54p slightly decreased the overall fraction of RNA that underwent splicing but increased the

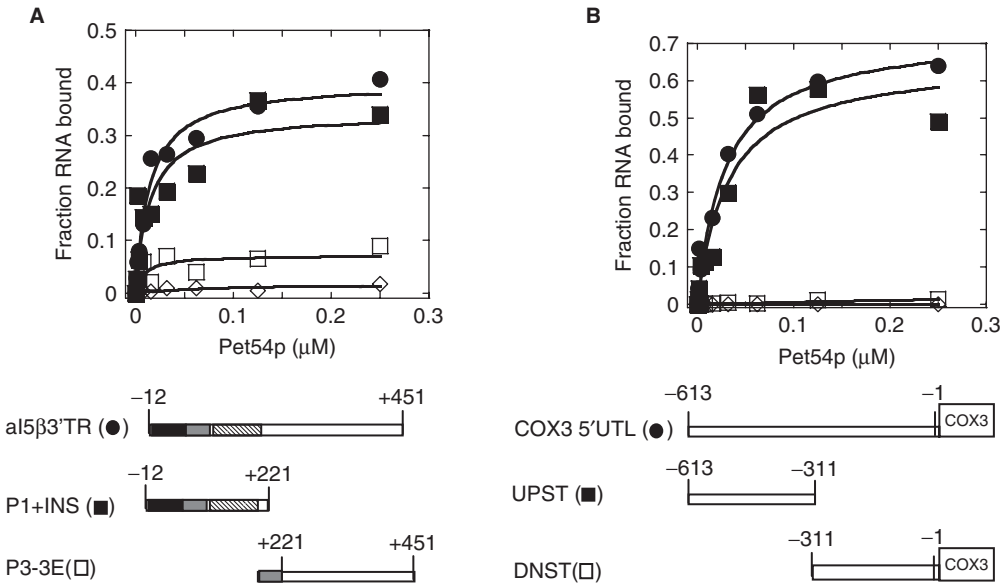

Figure 4. Pet54p binds with high affinity to subdomains within the COX3 5′ UTL and aI5β pre-RNA. In each experiment, trace amounts of internally ^{32}P-radiolabeled RNA was incubated with increasing amounts of Pet54p (0–500 nM) and complexes filtered onto nitrocellulose and the fraction of RNA bound calculated by the fraction of radioactivity retained on the filters versus the total filtered. The data were fit to an equilibrium binding equation (see Materials and Methods section). (**A**) Binding of aI5β 3′TR RNA and 5′ and 3′ truncations. As shown in the schematic, P1 + INS, contains 5′ exon through to the end of the insertion sequence; P3-3E, contains the intron core with the insertion sequence deleted. The open diamond symbols represent binding of the *A. nidulans* COB group I intron. In the schematic, the 5′ exon is black, the 5′ strand of P3 is gray and the insertion sequence is striped. (**B**) Binding of COX3 5′ UTL and 5′ and 3′ truncations. As shown in the schematic, UPST contains the first 302 nt of the UTL; DNST contains UTL sequence from A −312 to U −1. COX3 coding sequence (+1 and beyond) is shown for orientation but was not included in the RNAs tested. The open diamond symbols represent binding of the *A. nidulans* COB group I intron.

amplitude of ligated exons to 0.06 (± 0.002), a modest but reproducible increase of 1.5-fold (Figure 2B). The rate of ligation was not changed significantly by the addition of Pet54p (0.028 ± 0.007 versus $0.022 \pm 0.006\,min^{-1}$). Control experiments showed that Pet54p did not facilitate splicing in the absence of Mrs1p (data not shown). Thus, in the minimal aI5β *in vitro* splicing reaction, Pet54p appears to function primarily to increase the efficiency of exon ligation.

Overlapping binding sites in Pet54p for COX3 5′ UTL and COX1 aI5β containing RNAs

We performed UV cross-linking experiments (see above) to assess if Pet54p also directly interacts with the COX3 5′ UTL. Indeed, as with the aI5β pre-RNA, Pet54p formed an efficient crosslink with 4-thiouridine containing COX3 5′ UTL RNA (Figure 3A). To assess if the Pet54p used a single site for binding to the COX3 5′UTL RNA and COX1 aI5β containing RNAs, unlabeled competitor UTL and group I intron RNAs were included in the reaction mixture. Figure 3A shows that inclusion of unlabeled COX3 5′UTL, full length or truncated (aI5β 3′TR) aI5β RNAs abolished cross-linking of 4-thiouridine substituted COX3 5′UTL. In contrast, inclusion of the *A. nidulans* COB group I intron had no effect on cross-linking efficiency. Identical results were found for 4-thiouridine substituted aI5β 3′TR RNA (Figure 3B). Collectively, these observations provide evidence that Pet54p interacts specifically with both COX3 5′ UTL and aI5β pre-RNA. In addition, the ability of aI5β RNA to compete for binding to COX3 5′UTL and *vice versa* suggest that Pet54p contains a single or overlapping binding sites for each RNA.

Binding of COX3 5′ UTL and COX1 aI5β pre-RNA to Pet54p

To directly measure the binding affinity of Pet54p to its respective ligands and begin to delineate the RNA-binding sites, we carried out equilibrium binding assays on full length and truncated transcripts. For the aI5β 3′TR RNA (493 nt), Pet54p bound with a K_d^{app} of 18.3(± 6) nM while the *A. nidulans* COB intron showed little detectable binding (Figure 4A). Pet54p binds to the COX3 5′ UTL with a K_d^{app} of 20.8(± 8) nM, an affinity equal to that of the aI5β RNA (Figure 4B). The finding that Pet54p binds with similar affinity to the intron and UTL RNAs raises the possibility that Pet54p recognizes similar binding sites in both RNAs.

We next split the aI5β 3′TR RNA into two fragments to assess whether Pet54p bound within the aI5β group I intron catalytic core or to a region peripheral to the core. In this regard, a 233-nt RNA (P1 + INS) was synthesized that contained the 5′ exon through to the end of the idiosyncratic sequence that is inserted between the 5′ strands of P3 and P4 helices (Figures 1 and 4A). Pet54p bound this RNA bound with near wild-type affinity [K_d^{app} = 18.2(± 9) nM] providing evidence that the Pet54p recognizes sequences and/or structures within P1 through the insertion sequence (Figure 4A). In contrast, a 306-nt RNA (P3-3E) that contained the catalytic core of the intron (with the insertion sequence deleted), from P3

through the 3′ exon, was not appreciably bound by Pet54p (Figure 4A). These findings demonstrate that Pet54p does not bind to the intron catalytic core, but, instead, primarily recognizes the 5′ region of the aI5β RNA.

In a parallel analysis, the COX3 5′UTL was split into approximately equal-sized fragments containing the 5′ or 3′ halves of the RNA. Pet54p bound with ~2-fold decrease in affinity [K_d^{app} = 31.9(±3) nM) to an RNA fragment composed of the first 302 nt of the UTL (from A −613 to G −311; COX3UPST, Figure 4B). In contrast, Pet54p did not bind an RNA fragment containing the remaining UTL sequence from A −312 to U −1 (COX3DNST; Figure 4B). Thus, as in the case for the aI5β pre-RNA, Pet54p shows high affinity and selective binding to a subdomain within the COX3 5′ UTL.

Mapping the Pet54-binding site in COX3 5′ UTL and COX1 aI5β containing RNAs

The truncation experiments described above demonstrated that Pet54p bound to 5′ upstream regions in both COX3 5′ UTL and COX1 aI5β RNAs. To more precisely define the smallest 5′ fragment that can be bound by Pet54p, we employed a 'boundary assay' that has been used to map protein-binding sites in rRNA (e.g. 21). In these experiments, either 5′ end-labeled phosphorothioate (NαS)-substituted RNAs were treated with iodine that cleaves at each phosphorothioate linkage or unsubstituted RNA was treated with RNase T1 that cleaves after guanosine. In both cases, cleavage generates a number of fragments that are then incubated with protein. RNA fragments capable of binding protein are captured on a nitrocellulose filter, eluted and then separated on a denaturing gel. Comparison of the bound and unselected fragments identifies the shortest RNA capable of binding protein (21).

For 5′ end-labeled AαS substituted aI5β 3′TR RNA, Pet54p strongly bound RNAs that contained intron sequence up to A60, within the noncanonical insertion sequence (Figure 5A). Furthermore, Pet54p also bound fragments terminating at A50, but the reduced intensity of these bands relative to the other bound fragments is consistent with the protein having a reduced affinity for these RNAs. Taken together, these results show that virtually the entire intron catalytic core was not required for Pet54p binding and that the minimal 5′ terminal fragment bound by Pet54p is 62 nt. This includes 5′ exon (12 nt), the remainder of P1 helix, the 5′ strand of P3 and some sequences in the insertion sequence (50 nt total) of the aI5β RNA (see the schematics in Figures 1 and 6A).

The COX3 5′ UTL RNA is very A rich, and fragments generated from iodine cleavage of AαS substituted material were not sufficiently resolved by gel electrophoresis to accurately assign the identity of fragments bound to Pet54p. We therefore used CαS substituted RNA as well as T1-digested material. Experiments with cleaved CαS UTL RNAs showed that Pet54p bound 5′ end-labeled fragments that contained sequence up to C −410 while assays with the T1-digested material showed that Pet54p could also bind a shorter fragment terminating at G −476 (Figure 5B). Interestingly, COX3 5′UTL RNA

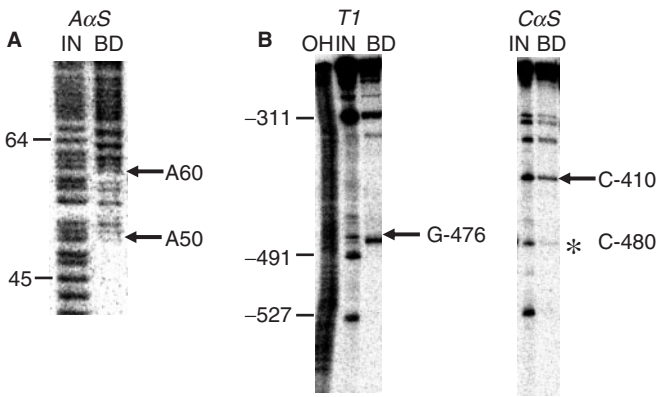

Figure 5. Mapping the Pet54p binding site on COX3 5′ UTL and COX1 aI5β containing RNA. (**A**) Boundary experiment for the aI5β 3′TR RNA. For 5′ end-labeled, AαS substituted aI5β 3′TR, Pet54p tightly bound RNAs fragments up to A60 and with lesser affinity to fragments terminated up to A50. IN, input; BD, Pet54p bound RNA. (**B**) Boundary experiment COX3 5′UTL RNA. For 5′ end-labeled UTL RNA digested with RNase T1, Pet54p tightly bound RNAs fragments terminated at G −476. For 5′ end-labeled CαS substituted COX3 5′UTL RNA, Pet54p tightly bound RNAs fragments up to C −410 and with significantly less affinity to fragments ending at C −480 (asterisk). OH, hydrolysis ladder.

terminated just upstream of G −476, at C −480, was poorly bound by Pet54p (see asterisk, Figure 5). This suggests that the 137-nt fragment defined by the first base of the UTL (A −613) and terminating at G −476 contains the Pet54p-binding site.

Footprinting the Pet54p-binding sites on the aI5β pre-RNA and COX3 5′ UTL

To identify the Pet54p-binding sites within the 5′ ends of both RNAs, RNA footprinting experiments were performed. The accessibility of the RNA ligands' phosphate backbones in the presence and absence of Pet54p was probed by partial ribonuclease digestion. The RNA was digested with the double-stranded specific RNase V1 while single-stranded regions were probed with RNase 1, and the results are shown in Figure 6. Interestingly, in both cases, Pet54p binding did not result in protection of any V1 cleavage sites, and, importantly, only a subset of RNase 1 cleavage sites were protected suggesting that Pet54p primarily binds single-stranded regions in both RNAs.

For the aI5β 3′TR pre-RNA, there were four regions of protection from RNase 1 digestion: within the P1 stem–loop, both in exon and intron sequences (from residues −g3 to A9), in the junction between P1 and P3 (J1/3; C22-A27) and in two segments of the insertion sequence (from A52 to U53 and U67 to A69; Figure 6A). Interestingly, positions −g3 to U3 are also cleaved with V1 consistent with these positions being base paired in the P1 helix (Figure 6A). The cleavage by both V1 and 1 RNases suggests that the paired and unpaired states of this helix are in dynamic equilibrium. The lack of protection from RNase V1 cleavage by protein binding may reflect that Pet54p-binding results in stabilization of the P1 helix while protection of positions in the P1 loop (A4–A9) may reflect direct binding by the protein. Interestingly, in the insertion

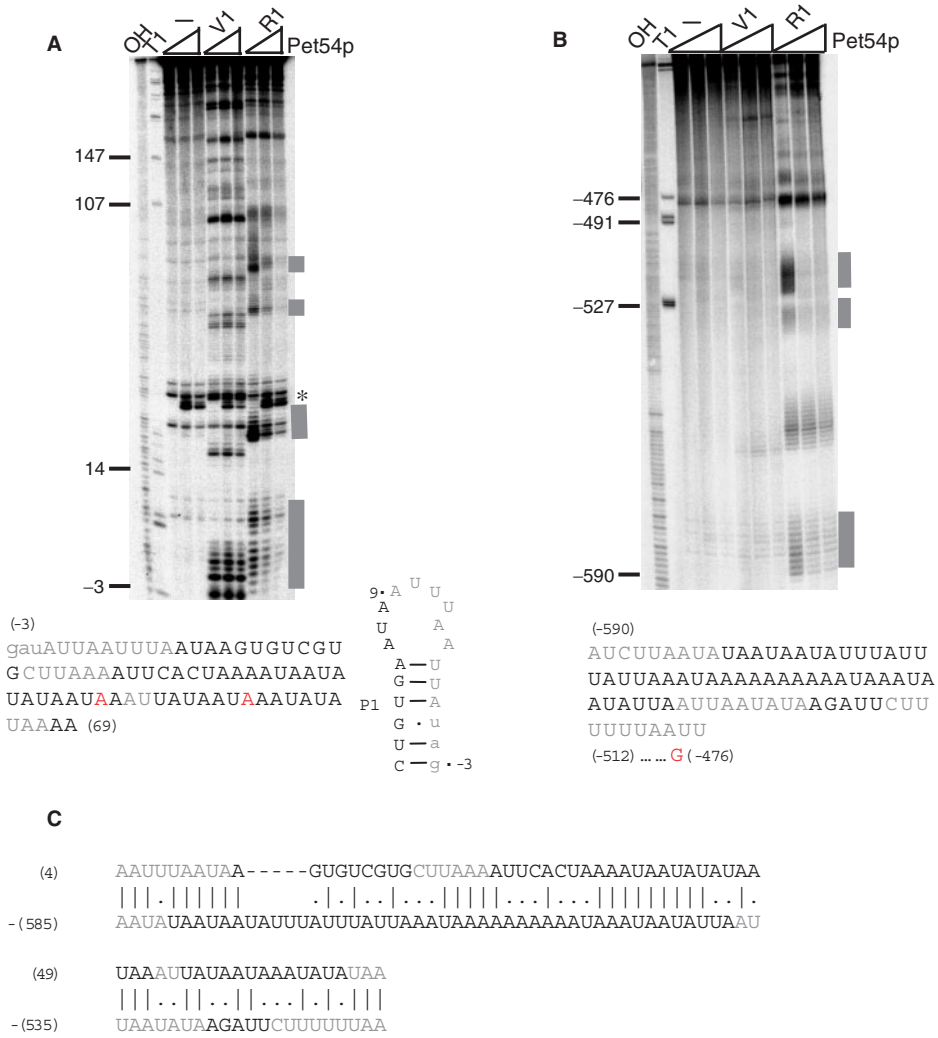

Figure 6. Visualization of the Pet54p-binding sites by RNase footprinting. 5′ end-labeled aI5β 3′TR RNA (**A**) or COX3 5′ UTL (**B**) were incubated with buffer (−), RNase V1 or 1 in the absence (first lane of each set) presence of saturating Pet54p (1.25 or 2.5 μM, second and third lanes of each set). Cleavage products were separated by denaturing gel electrophoresis and the data quantified as described in Materials and Methods section. Only those sites that showed 2-fold or higher reduction phosphorimager counts under both protein concentrations were identified as 'protected' (gray bars). Such sites were only observed in samples digested with RNase 1. The asterisk in (A) refers to bands of site-specific degradation caused by incubation with Pet54p. Below each gel image is a schematic of the relevant sequence protected from RNase1 digestion. Gray shading represents protection and the red shaded residues demarcate the 5′ binding boundary as defined in Figure 5. In (A), a secondary structure of the first 21 nt defining the P1 helix is also shown. Note that residues g −3 to U3 are also cleaved by the double-stranded specific V1 RNase, but Pet54p binding does not protect these residues from V1 cleavage. (**C**) Alignment of the RNase 1 protected sequence. The sequence from positions A4 to A69 of aI5β intron and positions A −590 to U −512 of the COX3 5′ UTL were aligned using the EBOSS program (32). Gray-shaded residues are protected from RNase 1 digestion in the presence of Pet54p [see (A) and (B) above].

sequence, the two regions protected from RNase 1 cleavage are both surrounded by regions cleaved by V1 suggesting that they are in loops or bulges within adjacent helices (Figure 6A).

Importantly, the protected regions lie within and adjacent to the sequences found to be critical for Pet54p binding in the boundary assay (Figure 5A). In this regard, the first two protected regions are within the minimal Pet54p bound 5′ fragment that terminated at A50 (shown in Figure 6A and see above). The third and fourth regions are just upstream and downstream of the high-affinity boundary, defined by the fragment ending at A60 (Figures 5A and 6A). Collectively, these results demonstrate that Pet54p-binding sites are within single-stranded regions close to the 5′ end of the aI5β RNA.

The COX3 5′UTL also showed multiple regions of protection from RNase 1 when bound to Pet54p (Figure 6B). Two of these regions (A −537 to A −529 and C −523 to A −512) are separated by only 5 nt, while the third region (A −590 to A −582) is further upstream. Poor V1 cleavage efficiency in this region of the RNA makes it difficult to judge the amount of secondary structure, however, given that RNase 1 cleaves only at selective positions suggests that the UTL contains significant secondary and/or tertiary structure. Presumably, the protected regions are close in the folded structure of the UTL.

The lengths of RNA containing the binding sites for aI5β (not including the P1 paired nts −3–3) and COX3 5′ UTL identified by RNase footprinting are of similar size (66 versus 78 nt, respectively) and the sequences are extremely AU rich (89% and 96%, respectively) suggesting that Pet54p may recognize related sequences in both RNAs. Indeed, alignment of these sequences show 56% identity (40/71), with the 5′ and 3′ boundaries of the protected fragments overlapping (Figure 6C). Although the 5′ most protected residues are not precisely aligned, both contain an AAUA sequence (Figure 6C). The 3′ most protected residues align at a UAA (Figure 6C). Interestingly, the protected sequence from C22 to A27 in aI5β RNA shares significant identity (67%) with the aligned COX UTL sequence. However, the lack of RNase 1 digestion in this region of the UTL prevents making strong conclusions about whether Pet54p binds to this region of the COX3 5′ UTL. Thus, while RNase footprinting analysis is restricted by a limited number of regions that show cleavage, these observations are consistent with Pet54p recognizing related sequences and/or structures within similar spatial constraints in both of its RNA ligands. These observations are reminiscent of the *E. coli* S7 and S15 ribosomal proteins that interact with different subdomains of 16S rRNA as well as their own mRNAs. In these cases, the RNA-binding sites are spread over a rather long, differently folded sequences that contain multiple, short (2–5 nt) stretches of strong identity (22–24).

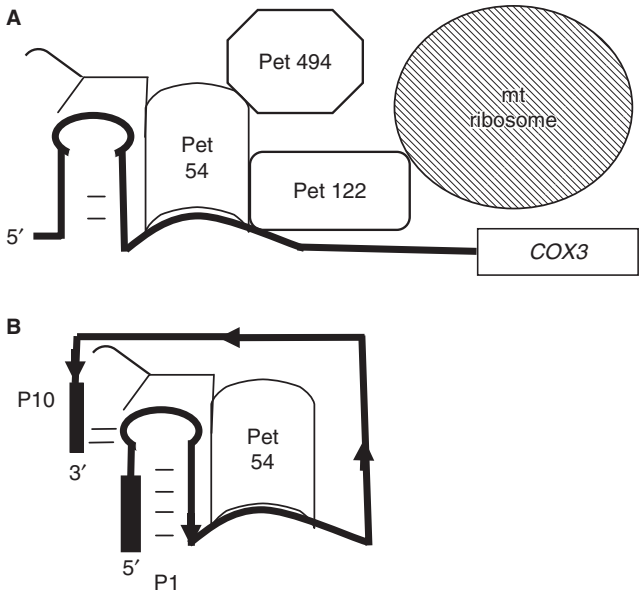

Figure 7. Model for Pet54p function in translational activation (**A**) and splicing (**B**). A common RNA-binding domain is used to interact with both RNAs, whereas different effector domains are required for each function. (A) The model for COX3 translational activation is adapted from references 8 and 31. The stem–loop shown is to emphasize that the UTL is likely structured but direct evidence for Pet54p binding to a stem–loop in the UTL is speculative (see Results section). (B) For the aI5β pre-RNA, the P1 and P10 interactions that position the exons (thick lines) into the catalytic core (thin lines with arrows) are emphasized. Interactions with the 3′ exon are shown to emphasize one possible model for Pet54p splicing function.

DISCUSSION

Pet54p cooperates with two distinct sets of proteins to activate COX3 translation and facilitate excision of the aI5β intron from the COX1 pre-mRNA. However, prior to this analysis, it was not known whether Pet54p was a specific RNA-binding protein, and if so, whether it recognized both of its ligands by a similar mechanism. In this study we show that recombinant Pet54p bound with high specificity and affinity to both the COX3 5′ UTL and aI5β pre-RNA in the absence of other cofactors demonstrating that it functions, in part, by interacting directly to both RNAs. Competition experiments were consistent with Pet54p using overlapping binding sites to interact with both RNAs. In support of this, we identified Pet54p-binding sites within the COX3 5′ UTL and aI5β pre-RNA by truncation experiments and RNase footprinting and showed that the sites are similar in spatial context and sequence. Collectively, these results suggest that Pet54p binds both RNAs in an analogous manner and, as discussed below, provides insight into the individual functions of Pet54p and its evolution as a splicing cofactor.

Translation activation of COX3

The protein products of the PET54, PET122 and PET494 genes are required for translation of the COX3 mRNA, and our results are consistent with Pet54p interacting directly with the 5′ UTL to mediate translational activation. Synthetic lethal and genetic suppression studies were consistent with a model in which Pet54p and Pet122p functionally interacts with the 5′ UTL of COX3, and mutational analysis has shown that an internal deletion between U −605 to A −406 of the 5′ UTL abolishes translational activation (8,25,26). Here we have shown that Pet54p physically interacts with the 5′ UTL of COX3, and furthermore, it specifically recognizes a 137-nt fragment (residues A −613 to G -476) that overlaps with the 199-nt region identified genetically to be important for COX3 translation. Furthermore, mutational analysis has also shown that deletion of COX3 5′UTL sequence from G −607 to G −527 severely diminish COX3 mRNA levels and protein production (26). The AU-rich segment (A −590 to U −512) that contains Pet54p-binding sites, as determined by RNase footprinting, overlaps this region. These results are consistent with Pet54p binding to the upstream region of the 5′ UTL and playing an important role in helping to assemble the activation complex onto an appropriate location within the COX3 mRNA to facilitate translation (8; Figure 7).

Splicing of the aI5β intron

Genetic analysis has shown that the protein products of MRS1, PET54, MSS18, MSS116 and SUV3 affect splicing of the aI5β intron, but whether all of these proteins act directly to facilitate splicing and what roles they play are unknown (3). We have shown that Mrs1p binding is sufficient to facilitate aI5β splicing *in vitro*, but the exon

ligation step is inefficient (Figure 2B; A.L. Bifano and M.G. Caprara, in preparation). Here we show that Pet54p binds with high specificity to the aI5β pre-RNA, and it associates primarily with the very 5′ end of the intron. Binding of Pet54p does not facilitate general catalytic activity of the aI5β intron *in vitro*, but, instead, increases the efficiency of the exon ligation step. The increase in the fraction of molecules that undergo the second step is a modest ~1.5-fold suggesting that other factors may collaborate with Pet54p to assist in this step. While the mechanism of action is still under investigation, the finding that Pet54p binds to the 5′ end of aI5β raises the possibility that it may assist in stabilizing the interaction of the 3′ exon with the intron's internal guide sequence (P10 pairing) that serves to position the 3′ SS for ligation after the first step in splicing (Figure 7; 12). On the other hand, results from the RNase mapping experiments suggests that binding of Pet54p also stabilizes pairing of the 5′ exon to the internal guide sequence (P1 pairing). Thus, Pet54p may assist in splicing by preventing premature dissociation of the 5′ exon after the first step in splicing.

Previously it was shown by northern analysis that aI5β containing COX1 pre-mRNAs accumulated in PET54 disruption strains suggesting that the protein also is important in the first splicing step (6). Presumably our *in vitro* conditions mask this contribution of Pet54p in splicing. However, given that Pet54p binding appears to stabilize the P1 pairing, it may act by promoting docking of the 5′ exon into the intron's catalytic core. Regardless of the specific mechanism, the observation that Pet54p interacts near (or at) the SSs makes it unique among characterized group I intron cofactors, which primarily bind to and stabilize the active structure of the intron core (3,14–17).

Evolutionary implications

Our findings show that Pet54p uses the same or overlapping binding sites to interact with the COX3 5′ UTL and the aI5β intron and a part of the recognition involves related features that span ~60 nt in both RNAs. Given that splicing is likely a secondary adaptation of the protein (see Introduction section), these observations support a model in which Pet54p became involved in aI5β processing by virtue of a fortuitous interaction with sequences and/or structures in the intron that resembled its native recognition site in COX3 5′ UTL. A specific function for Pet54p may have been selected over time if changes in the protein increased the efficiency of splicing. It would be essential that these changes did not impair Pet54p translational activation function; thus, in this model, 'effector domains' of Pet54p are predicted to be separate. In support of this hypothesis, mutations that affect one or the other function have been discovered providing evidence that both functions of Pet54p are genetically separable (27). Together with our data, this latter observation suggests that the splicing function of Pet54p may include both RNA binding and effector domains (Figure 7).

Group I intron cofactors either use pre-existing nucleic acid-binding sites to facilitate splicing or 'develop' new binding sites from nonfunctional surfaces. For example, a conserved RNA-binding domain in the yeast mt leucyl-tRNA synthetase is critical for its role in aminoacylation, as well as promoting splicing of bI4 intron (28). In contrast, the homing endonuclease I-AniI from *Aspergillus* and the mt tyrosyl tRNA synthetase from *Neurospora* both have developed independent group I intron RNA-binding sites (29–31). The Pet54p protein appears to have traveled a unique evolutionary path. On the one hand, it uses a pre-existing RNA-binding site for binding to the aI5β intron, but another, yet to be defined surface, is primarily important for splicing and not translational activation. Thus, in other cases, the evolution of coordinated gene expression at the RNA level may similarly involve the development of protein cofactors that use a single recognition mechanism for two or more substrates, with binding regulating different steps in the expression of individual genes.Continuing studies of the structure and functions of Pet54p should provide new insights into how RNA-binding proteins, in general, may be exploited for other functions *in vivo*.

ACKNOWLEDGEMENTS

We thank Dr E. Turk (CWRU) for critical reading of the manuscript, as well as the critical comments of two anonymous reviewers. B.J.K. was supported in part by a Cell and Molecular Biology Training Grant awarded through NIGMS. National Institutes of Health grant GM-62853 to M.G.C. supported this work. The Open Access charges for this paper were waived by Oxford University Press.

Conflict of interest statement. None declared.

REFERENCES

1. Haugen,P., Simon,D.M. and Bhattacharya,D. (2005) The natural history of group I introns. *Trends Genet.*, **21**, 111–199.
2. Foury,F., Roganti,T., Lecrenier,N. and Purnelle,B. (1998) The complete sequence of the mitochondrial genome of Saccharomyces cerevisiae. *FEBS Lett.*, **440**, 325–331.
3. Lambowitz,A.M., Caprara,M.G., Zimmerly,S. and Perlman,P.S. (1999) Group I and group II ribozymes as RNPs: clues to the past and guides to the future. In Gesteland,R.F., Atkins,J.F. and Cech,T.R. (eds), *The RNA World II*. Cold Spring Harbor Laboratory Press, New York, pp. 451–485.
4. Valcarcel,J. and Gebauer,F. (1997) Post-transcriptional regulation: the dawn of PTB. *Curr. Biol.*, **7**, R705–R708.
5. Sanford,J.R., Ellis,J. and Caceres,J.F. (2005) Multiple roles of arginine/serine-rich splicing factors in RNA processing. *Biochem. Soc. Trans.*, **33**, 443–446.
6. Valencik,M.L., Kloeckener-Gruissem,B., Poyton,R.O. and McEwen,J.E. (1989) Disruption of the yeast nuclear PET54 gene blocks excision of mitochondrial intron aI5 beta from pre-mRNA for cytochrome c oxidase subunit I. *EMBO J.*, **8**, 3899–3904.
7. Costanzo,M.C., Seaver,E.C. and Fox,T.D. (1986) At least two nuclear gene products are specifically required for translation of a single yeast mitochondrial mRNA. *EMBO J.*, **5**, 3637–3641.
8. Brown,N.G., Costanzo,M.C. and Fox,T.D. (1994) Interactions among three proteins that specifically activate translation of the mitochondrial COX3 mRNA in Saccharomyces cerevisiae. *Mol. Cell. Biol.*, **14**, 1045–1053.

9. Fox,T.D. (1996) Translational control of endogenous and recoded nuclear genes in yeast mitochondria: regulation and membrane targeting. *Experientia*, **52**, 1130–1135.
10. Haffter,P., McMullin,T.W. and Fox,T.D. (1991) Functional interactions among two yeast mitochondrial ribosomal proteins and an mRNA-specific translational activator. *Genetics*, **127**, 319–326.
11. Chacinska,A. and Boguta,M. (2000) Coupling of mitochondrial translation with the formation of respiratory complexes in yeast mitochondria. *Acta Biochim. Pol.*, **47**, 973–991.
12. Hougland,J., Piccirilli,J., Forconi,M., Lee,J. and Herschlag,D. (2005) How the group I intron works: a case study of RNA structure and function. In Gesteland,R.F., Cech,T.R. and Atkins,J.F. (eds), *The RNA World*, Vol. 3, Cold Spring Harbor Laboratory Press, New York, pp. 133–205.
13. Woodson,S.A. (2005) Structure and assembly of group I introns. *Curr. Opin. Struct. Biol.*, **15**, 324–330.
14. Caprara,M.G., Mohr,G. and Lambowitz,A.M. (1996) A tyrosyl-tRNA synthetase protein induces tertiary folding of the group I intron catalytic core. *J. Mol. Biol.*, **257**, 512–531.
15. Weeks,K.M. and Cech,T.R. (1995) Protein facilitation of group I intron splicing by assembly of the catalytic core and the 5′ splice site domain. *Cell*, **82**, 221–230.
16. Ho,Y. and Waring,R.B. (1999) The maturase encoded by a group I intron from Aspergillus nidulans stabilizes RNA tertiary structure and promotes rapid splicing. *J. Mol. Biol.*, **292**, 987–1001.
17. Caprara,M.G., Chatterjee,P., Solem,A., Brady- Passerini,K.L. and Kaspar,B.J. (2007) An allosteric-feedback mechanism for protein assisted group I intron splicing. *RNA*, **13**, 211–222.
18. Solem,A., Chatterjee,P. and Caprara,M.G. (2002) A novel mechanism for protein-assisted group I intron splicing. *RNA*, **8**, 412–425.
19. Emerick,V.L., Pan,J. and Woodson,S.A. (1996) Analysis of rate-determining conformational changes during self-splicing of the Tetrahymena intron. *Biochemistry*, **35**, 13469–13477.
20. Golden,B.L. and Cech,T.R. (1996) Conformational switches involved in orchestrating the successive steps of group I RNA splicing. *Biochemistry*, **35**, 3754–3763.
21. Ryan,P.C. and Draper,D.E. (1989) Thermodynamics of protein-RNA recognition in a highly conserved region of the large-subunit ribosomal RNA. *Biochemistry*, **28**, 9949–9956.
22. Robert,F. and Brakier-Gingras,L. (2001) Ribosomal protein S7 from Escherichia coli uses the same determinants to bind 16S ribosomal RNA and its messenger RNA. *Nucleic Acids Res.*, **29**, 677–682.
23. Nikulin,A., Serganov,A., Ennifar,E., Tishchenko,S., Nevskaya,N., Shepard,W., Portier,C., Garber,M., Ehresmann,B., Ehresmann,C. *et al.* (2000) Crystal structure of the S15-rRNA complex. *Nat. Struct. Biol.*, **7**, 273–277.
24. Philippe,C., Bénard,L., Portier,C., Westhof,E., Ehresmann,B. and Ehresmann,C. (1995) Molecular dissection of the pseudoknot governing the translational regulation of Escherichia coli ribosomal protein S15. *Nucleic Acids Res.*, **23**, 18–28.
25. Costanzo,M.C. and Fox,T.D. (1993) Suppression of a defect in the 5′ untranslated leader of mitochondrial COX3 mRNA by a mutation affecting an mRNA-specific translational activator protein. *Mol. Cell. Biol.*, **13**, 4806–4813.
26. Wiesenberger,G., Costanzo,M.C. and Fox,T.D. (1995) Analysis of the Saccharomyces cerevisiae mitochondrial COX3 mRNA 5′ untranslated leader: translational activation and mRNA processing. *Mol. Cell. Biol.*, **15**, 3291–3300.
27. Valencik,M.L. and McEwen,J.E. (1991) Genetic evidence that different functional domains of the PET54 gene product facilitate expression of the mitochondrial genes COX1 and COX3 in Saccharomyces cerevisiae. *Mol. Cell. Biol.*, **11**, 2399–2405.
28. Rho,S.B., Lincecum,T.L.,Jr. and Martinis,S.A. (2002) An inserted region of leucyl-tRNA synthetase plays a critical role in group I intron splicing. *EMBO J.*, **21**, 6874–6881.
29. Chatterjee,P., Brady,K.L., Solem,A., Ho,Y. and Caprara,M.G. (2003) Functionally distinct nucleic acid binding sites for a group I intron encoded RNA maturase/DNA homing endonuclease. *J. Mol. Biol.*, **329**, 239–251.
30. Bolduc,J.M., Spiegel,P.C., Chatterjee,P., Brady,K.L., Downing,M.E., Caprara,M.G., Waring,R.B. and Stoddard,B.L. (2003) Structural and biochemical analyses of DNA and RNA binding by a bifunctional homing endonuclease and group I intron splicing factor. *Genes Dev.*, **17**, 2875–2888.
31. Paukstelis,P.J., Coon,R., Madabusi,L., Nowakowski,J., Monzingo,A., Robertus,J. and Lambowitz,A.M. (2005) A tyrosyl-tRNA synthetase adapted to function in group I intron splicing by acquiring a new RNA binding surface. *Mol. Cell.*, **17**, 417–428.
32. Rice,P., Longden,I. and Bleasby,A. (2000) EMBOSS: The European Molecular Biology Open Software Suite. *Trends Genet.*, **16**, 276–277.